Separations: Materials, Devices and Processes

Synthesis and Application of Ethylenediamine Tetrapropionic Salt as a Novel Draw Solute for Forward Osmosis Application

Qingwu Long, Guangxian Qi, and Yan Wang
Key Laboratory for Large-Format Battery Materials and System, Ministry of Education, School of Chemistry and Chemical Engineering, Huazhong University of Science and Technology, Wuhan 430074 China

DOI 10.1002/aic.14720
Published online January 10, 2015 in Wiley Online Library (wileyonlinelibrary.com)

The development of suitable draw solutes for forward osmosis (FO) process is a big obstacle on the way of its real industrialization. In this work, a novel draw solute, ethylenediamine tetrapropionic (EDTP) acid (salt) is developed for FO application. The successful synthesis is confirmed by Fourier transform infrared spectroscopy, nuclear magnetic resonance spectroscopy, and high resolution mass spectrum. By optimizing the pH of EDTP solution, its composition is varied, and therefore, its water solubility and osmotic pressure are effectively improved. The effects of EDTP concentration on the osmotic pressure and FO performance are also investigated. Its outstanding osmotic pressure and big molecular size result in a high water flux of 22.69 LMH and a low salt flux of 0.32 gMH with 0.8 M EDTP draw solution (water as the feed solution, pressure retarded osmosis mode). The good stability and easy recovery by nanofiltration of EDTP solution also demonstrate its great potential as the draw solute for future FO applications. © 2015 American Institute of Chemical Engineers *AIChE J*, 61: 1309–1321, 2015

Keywords: forward osmosis, draw solution, synthesis, ethylenediamine tetrapropionic acid, osmotic pressure, membrane separation

Introduction

In the past few decades, various technologies have been developed for seawater desalination and wastewater reuse to alleviate the severe water shortage problem. Especially, the membrane-oriented separation technologies, including reverse osmosis (RO), nanofiltration (NF), membrane distillation (MD), and so forth.[1–6] are popular for providing a steady supply of clean water without impairing or straining natural fresh water ecosystems.[7] However, all above technologies are still inherently energy-intensive. It is, therefore, imperative to develop some more robust and energy efficient desalination technologies for water reuse. Forward osmosis (FO) has emerged as an attractive membrane technology recently for water recovery and treatment, owing to its high recovery, low fouling tendency, high energy efficiency, and so forth.[8–10] It is expected to become a potential alternative technology to alleviate the stress of freshwater scarcity in the future.

Despite of the superior advantages of FO technology, its development is still hindered by the selection of suitable FO membranes and the limited choice of available draw solutes.[11] Numerous previous researches have focused on the fabrication of high-performance FO membranes (e.g., thin film composite membrane, layer by layer membrane) to reduce the effects of internal concentration polarization (ICP), reverse salt diffusion, antifouling, and so forth.[12–19] While the lack of suitable draw solution with high osmotic pressure and easy recovery ability is still the big obstacle on the way of FO industrialization. In recent years, more attention has gradually been paid on the exploration of novel draw solutes.[20]

Table 1 lists some common draw solutes used in FO process. In the early studies, conventional inorganic salts or organic molecules including NaCl, $MgCl_2$, and sugar are extensively investigated with resultant reasonably high water fluxes in FO process. However, their high reverse salt flux is always the major obstacle for their further development. Later, some natural products (e.g., glucose[21] and amino acid[22]) were used as the draw solutes in FO process. Recent progresses on synthetic draw solutes, such as thermolytic salts,[23–26] hydracids complexes,[27] "dendrimer-like" compounds,[28,29] polyelectrolytes,[30] "smart-type" magnetic nanoparticles,[31] and stimuli–responsive hydrogels[32] were also explored as novel draw solutes in FO process for their high osmotic pressure, high water flux, and reasonable draw solute rejection. However, the severe reverse salt flux of thermolytic salts, possible biodegradation of organic compounds and agglomeration of magnetic nanoparticles limit their applications as draw solutes, since a low water flux could be resulted with the diminished osmotic pressure.[31,33,34] Investigation of some novel synthetic compounds as draw solutes have always been the research focus of FO scientists in recent years, especially the carboxyl-containing organic draw solutes.[30,35,36] Because their high osmotic pressure and expanded molecular structure, a high water flux and a

Additional Supporting Information may be found in the online version of this article.

Correspondence concerning this article should be addressed to Yan Wang at wangyan@hust.edu.cn

Table 1. Benchmarking with Previously Reported Draw Solutes for FO Applications

Draw solute	Osmotic pressure (bar)	Feed	Membrane	Water flux (LMH)	Reverse salt flux (gMH)	Regeneration method	Ref.
EDTP sodium 0.8 M	118.14	DI water, 25°C, pH 8 0.3 mL min^{-1}	HTI-CTA flat sheet membrane	22.69 PRO	0.32	NF	This work
EDTP sodium 0.6 M	77.14	DI water, 25°C, pH 8 0.3 mL min^{-1}	HTI-CTA flat sheet membrane	18.6 PRO	0.26	NF	
Glycine, 1.24 M	24.2	DI water, 21±2°C, 6.25 L min^{-1}	HTI-CTA flat sheet membrane	~5 PRO	2.13	–	22
EDTA sodium, 0.8 M	85.77 [a]	DI water, 23°C, pH 8 384 cm min^{-1}	HTI-CTA flat sheet membrane	~12.9 PRO	~0.32	–	28
Sodium lignin sulfonate, 600 g/1000 g water	78.23	DI water, 23°C	HTI-CTA flat sheet membrane	8 FO 15 PRO	26	No need	40
Hydroacid complexes Fe-CA, 1.0 M	–	DI water	HTI-CTA flat sheet membrane	11 FO 21 PRO	0.1–0.2	NF	27
Hexavalent phosphazene salts, 0.5 M	52	DI water,30°C	HTI-CTA flat sheet membrane	~7 FO	–	Not studied	29
Sodium propionate, 1.06 M	42	DI water, 25°C, 1.5 L min^{-1}	HTI-CTA flat sheet membrane	10.69 FO	2.29	RO	35
Polyelectrolyte PAA-Na 1800	55	DI water, 25°C	HTI-CTA flat sheet membrane	19 PRO	–	Ultrafiltration	30
Sucrose, 1 M	26.7	DI water	CA hollow fiber	12.9 FO	–	–	21
$MgCl_2$, 2 M	93.7	DI water	CA hollow fiber	17.1 PRO	–	–	21
NaCl, 0.87 M	42	DI water, 25°C, 1.5 L min^{-1}	HTI-CTA flat sheet membrane	12.17 FO	–	–	21
NH_4HCO_3, 1.1 M	42	DI water	HTI-CTA flat sheet membrane	10.26 FO	–	–	23,24
2-Methylimidazole based solutes, 1 M	70	DI water	HTI-CTA flat sheet membrane	13 PRO	–	Membrane Distillation	46
Surface-functionalized Magnetic nanoparticles, 0.05 M	37.76	DI water, 22°C	HTI-CTA flat sheet membrane	7.5 FO 12 PRO	–	Magnetic field	31,33

[a]The osmotic pressure of EDTA sodium solution was tested at pH 8 by ourselves.

relative low salt flux can be expected. Recently, Hau et al.[28] and Zhao et al.[36] successfully used carboxyl-containing ethylenediamine tetraacetic acid (EDTA) and some dendrimers as draw solutes in FO application, respectively. The result shows a superior FO performance as compared with most previously reported draw solutes. It may, therefore, provide a new thought to design the next-generation draw solutes for FO process.

In this study, a novel tetracarboxyl compound—ethylenediamine tetrapropionic (EDTP) acid/salt is synthesized and explored as the draw solute for FO application. Since EDTP compound has a unique chemical structure, which makes it to be modified easily by iterative method for the synthesis of dendrimers or other macromolecules, the synthesis of EDTP could, therefore, be the research basis of the future study of mini or mid-scale dendrimers as FO draw solutes. EDTP acid (Figure 1) was synthesized by a simple three-step procedure as displayed in Scheme 1. Chemical structures of synthesized compounds are fully characterized by Fourier transform infrared spectroscopy (FTIR), nuclear magnetic resonance spectroscopy (NMR), and high resolution mass spectrum (HRMS). The pH of the EDTP sodium solution is optimized to investigate the effect of the solution composition on the resultant osmotic pressure and FO performance. The effect of the draw solute concentration and its stability have also been evaluated. The recovery of diluted draw solution after FO tests is carried out through a pressure-driven NF membrane process. It is envisioned that this study may provide further insight into the future research direction for the development of "ideal" organic draw solutes.

Experimental

Materials and chemicals

Reagents used in this work, methyl acrylate (MA, ≥98%), ethylenediamine (EDA, >99%), methanol (CH_3OH, >99.5%), sodium hydroxide (NaOH, 99%), sodium chloride

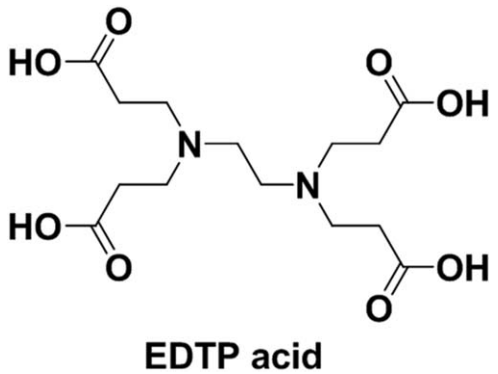

Figure 1. Structure of ethylenediaminetetrapropionic acid (EDTP acid).

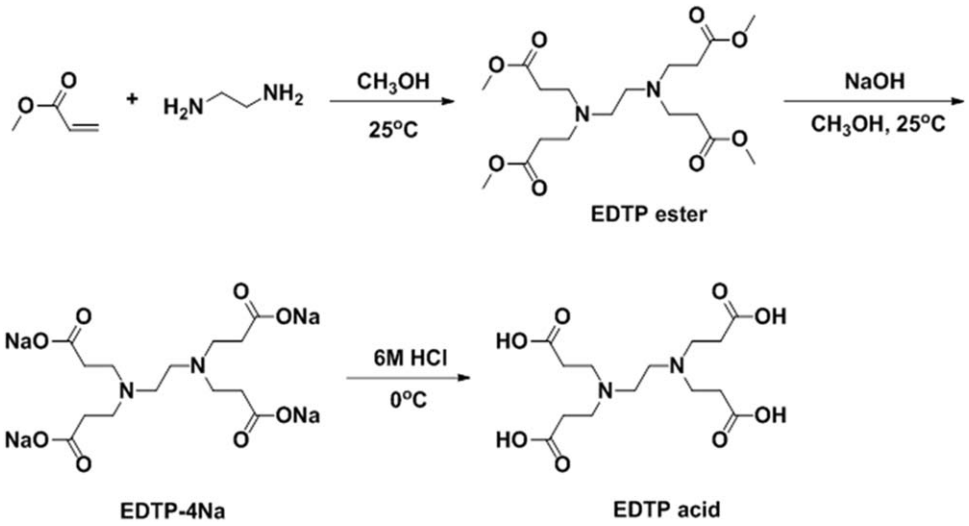

Scheme 1. Synthetic route of EDTP acid.

(NaCl, 99.5%), EDTA (99%), and concentrated hydrochloric acid (HCl, 37%) were all supplied from Sino-pharm Chemical Reagent Co. Before use, MA was treated by a chromatography column filled with aluminum oxide to remove polymerization inhibitor, while EDA was fully dried with activated molecular sieves. Others were used as received. Pouch-type flat-sheet FO membrane with cellulose triacetate (CTA) casted on woven substrate was provided by Hydration Technologies Inc. (HTI).[37] The deionized water used in FO test was generated in lab by a Wuhan Pin Guan Ultrapure LAB system with a resistivity of 18.25 MΩ cm.

Synthesis and characterization of EDTP acid

EDTP acid was synthesized by a three-step reaction as shown in Scheme 1. First, methyl ethylenediamine tetrapropionate (EDTP ester) was generated by Michael addition reaction according to the literature.[38,39] In a typical experiment, 0.1 mol EDA and 40 mL of dry methanol were placed in a 250 mL three-neck round-bottom flask. The mixture was cooled to 0°C and degassed for about 30 min. Then, a solution of 0.8 mol MA in 60 mL methanol was added slowly through a constant pressure dropping funnel under nitrogen protection. The resulted solution was kept in dark and stirred at room temperature for 7 days. The reaction mixture was then concentrated under reduced pressure with rotary evaporator to remove methanol and redundant MA. The crude product was further dried in a vacuum oven at 60°C for 5 h to yield a colorless oil product—EDTP ester. The yield is about 97%.

In the second step, sodium ethylenediamine tetrapropionate (EDTP-4Na) was obtained by hydrolysis of the ester product, with sodium hydroxide as the base and methanol as the solvent.[38] First, NaOH (0.5 mol) was dissolved in 150 mL methanol and cooled to 0°C. Then, EDTP ester (0.1 mol) was diluted by being added into 50 mL dry methanol and the obtained mixture was slowly added to above NaOH solution below 5°C for 1 h. The reaction solution was refluxed and stirred under mechanical agitation for 5 h. The crude reaction mixture was then filtered with a Buchner funnel, and the filtrated cake was washed with dry methanol (30 mL each for twice), followed by further dry in a vacuum oven at 60°C for 5 h to yield the white solid product—EDTP-4Na. The yield is about 91%.

To enhance the product purity, EDTP-4Na was further converted to EDTP acid in the last step. 0.1 mol EDTP-4Na was dissolved in 60 mL deionized water, and the solution was stirred and cooled to 0°C. A 6 M HCl solution was added to adjust the pH of EDTP-4Na solution to around 2. Then, a white precipitate was formed in this process. The mixture was stirred for another 30 min. The solvent was removed by filtration, and the crude solid was washed with deionized water for three times to yield a white solid product—EDTP acid. The yield is about 92%.

The as-synthesized structures are examined by NMR and HRMS spectra. ^{1}H and ^{13}C NMR spectra are recorded on Bruker AVANCE III 400 MHz Instrument. $CDCl_3$ with tetramethylsilane as an internal standard and D_2O were used as deuterated reagent for the NMR test. HRMS spectra are measured on a Bruck micrOTOF-Q instrument. FTIR spectra were recorded with a Brucker VERTEX-70 spectrophotometer with the range of 4000–400 cm^{-1} wavenumbers. The melting points of synthesized chemicals were detected by the Melting Point Instrument (X-4, YUHUA instrument).

Preparation of EDTP sodium salts draw solution

To have a suitable draw solute with a good solubility and osmotic pressure, the composition of the EDTP acid/salt solution is optimized via pH adjustment. With the addition of 1 M NaOH (2.75–3.05 mL) into 0.2 M EDTP acid solution (a turbid solution), the resulted EDTP sodium solutions will exhibit various pH values (6–8). The pH value of their aqueous solutions were measured by a pH meter (Sartorius AG, UB-7) and listed in Table 2. The water solubility of the EDTP solute was also measured at 25°C. All EDTP sodium solution was further purified by the dialysis bag with molecular weight cut off (MWCO) of 100 Da before use.

Measurement of osmotic pressure and relative viscosity

In this work, the freezing point depression method was used to determine the osmotic pressure of EDTP sodium solutions.[40] Freezing point depression is a general colligative property of the dilute solution, where its freezing point

Table 2. Basic Properties of EDTP Acid and Sodium Salts

	EDTP acid	EDTP-Na	EDTP-2Na	EDTP-3Na	EDTP-4Na
Chemical structure	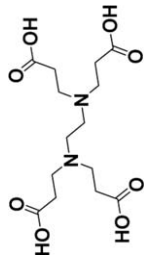	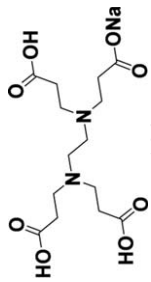	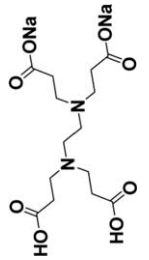	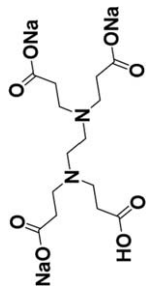	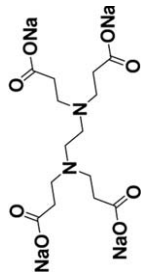
pH value of 0.2 M solution 23 °C)	1.99	4.86	5.42	8.64	12.33

decreases when another compound is added. The freezing point depression was measured using a lab-scale set-up (Figure 2), which is assembled by a freezer (down to −20°C), a platinum resistance thermometer (Cole-Parmar 90080-12, with an accuracy of ±0.05°C) to record the temperature profile, and a computer to export data. From the temperature curve, we can obtain the freezing points of pure water (T_0) and the solution (T_t). The freezing point depression value ($\Delta T = T_0 - T_t$) in NaCl, EDTA, and EDTP solutions of various concentrations (0.1–0.8 M) were recorded and the corresponding osmotic pressures (π) were calculated according to Eq. 1

$$\pi = \frac{\Delta T}{1.86} \times 22.66(\text{bar}) \tag{1}$$

A linear relationship between ΔT and the solution concentration C was obtained ($\Delta T = 3.53748C - 0.05117$, $R^2 = 0.9982$). This phenomenon is consistent with previous reported literature data.[40]

The relative viscosity of draw solutions (against DI water) was determined by an Ubbelohde viscometer. The operating temperature of 25°C was maintained by a temperature-controlled water bath in the lab according to the previous work.[30]

FO performance experiments

FO test was carried out through a bench-scale FO–NF coupled system as depicted in Figure 3. Before experiment, the HTI membrane was stabilized by being soaked in DI water for 30 min to remove glycerin on membrane surface. The membrane with an effective membrane area of 18.9 cm^2 was placed in a membrane cell with the rectangular channel size of 9 × 2.1 × 0.23 (length × width × depth) cm on each side of the membrane. Both the feed and draw solution side flow cocurrently through respective cell channels at the same flow rate of 0.3 L min^{-1} driven by two peristaltic pumps (Changzhou Kejian, BT00–600 M). DI water as the feed solution and the synthesized EDTP sodium solution as the draw solution were maintained at a temperature of 25 ± 0.5°C during all FO tests. A balance (AND, EK4100i) was used to monitor the weight change of the draw solution and a computer to export the data every 30 s. All FO tests were performed for 30 min each time. The FO tests are operated in two different modes, that is, FO mode (rejection layer contacting feed solution) and pressure retarded osmosis (PRO) mode (rejection layer contacting draw solution). The water flux J_w (L m^{-2} h^{-1}, noted as LMH) was calculated from the weight change of the draw solution according to Eq. 2

$$J_w = \frac{\Delta m}{\rho A \Delta t}(\text{LMH}) \tag{2}$$

where Δm (g) is the weight change of the draw solution after a predetermined time Δt (h), A is the active membrane area (m^2), and ρ is the water density.

The salt flux J_s (g m^{-2} h^{-1}, noted as gMH) was calculated from the concentration change of the feed solution according to Eq. 3

$$J_S = \frac{C_t V_t - C_0 V_0}{A \Delta t} \quad (\text{gMH}) \tag{3}$$

where C_0 and C_t (mg L^{-1}) are the initial feed concentration and that after a predetermined operation time Δt (h), which

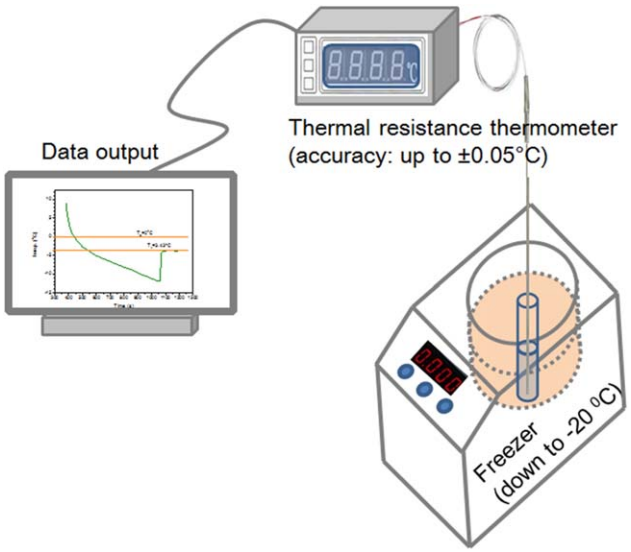

Figure 2. The bench-scale system of freezing point determination.

[Color figure can be viewed in the online issue, which is available at wileyonlinelibrary.com.]

are measured by a calibrated conductivity meter (Mettler toledo, FE30) at total dissolved solids (TDS) mode directly. V_0 and V_t (L) are the initial feed volume and volume after a predetermined time Δt.

With time passing by, the draw solution will be diluted. It is therefore necessary to supplement a fresh EDTP salt into the draw solution to maintain the constant concentration. The supplemented amount of EDTP salt is calculated according to the following Eq. 4

$$m_{supp} = \frac{\Delta m}{\rho_{water}} \times C_{draw} \quad (4)$$

where Δm is the mass increment of draw solution during testing time, ρ_{water} is the water density ($\sim$1000 g L^{-1}), and C_{draw} (g L^{-1}) is the initial concentration of the draw solution.

Recovery of EDTP sodium dilute solution

A pressure-driven NF setup (SuZhou Faith & Hope Membrane) was used to regenerate the diluted EDTP sodium draw solute after FO test. The feed solution used is 0.01 M EDTP solution diluted from 0.2 M draw solution (pH 8), and the upstream pressure is 1 bar. Polybenzimidazole NF membranes with MWCO of 400 Da (SuZhou Faith & Hope Membrane) were used. A pure water flux of 0.73 LMH bar^{-1} can be obtained with this membrane under an upstream pressure of 1 bar. The salt rejection of the NF system that indicates the capability of membrane isolation against to the draw solute was calculated by Eq. 5

$$R = \left(1 - \frac{C_p}{C_f}\right) \times 100\% \quad (5)$$

where C_p (mg L^{-1}) and C_f (mg L^{-1}) are the solute concentration in the permeate and the feed solution, respectively, and detected via a calibrated conductivity meter (Mettler toledo, FE30) at TDS mode directly.

Results and Discussion

Synthesis and characterization of EDTP acid

As mentioned in the experimental part, EDTP acid was synthesized via a three-step reaction route (Scheme 1). The water solubility test shows that the as-synthesized EDTP acid has a very low water solubility (<1 g), significantly lower than that of EDTP-4Na (>100 g). The maximum amount of EDTP acid in the solution can be obtained by adjusting the solution pH to 2 as determined by the dissociation constant (pKa = 3.00) of EDTP acid.[41]

To confirm the successful synthesis of EDTP ester, salt (EDTP-4Na), and acid, chemical structures of the obtained compounds are examined by NMR, HRMS, and IR. The ^{1}H NMR and ^{13}C NMR spectra in Figures 4 and 5 both show a structural evolution of EDTP compound, respectively. In the ^{1}H NMR spectra, the peak of methylene groups (—CH_2—) splits into two triplets, which could be ascribed to the two methylene groups on —NCH_2CH_2CO— structure with different chemical environment. The one nearer to the N-terminal

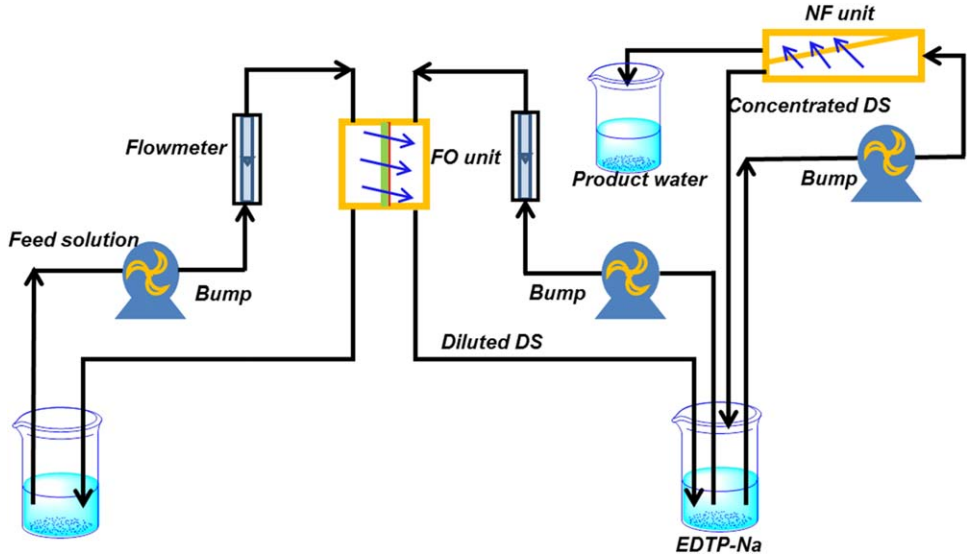

Figure 3. Schematic diagram of the lab-scale FO−NF system.

[Color figure can be viewed in the online issue, which is available at wileyonlinelibrary.com.]

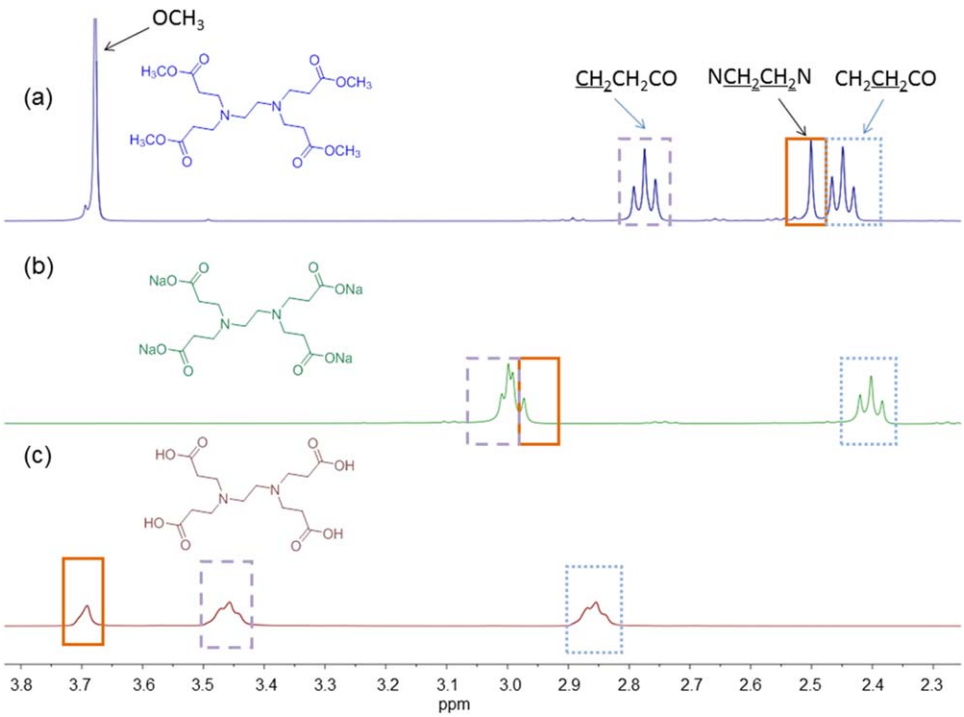

Figure 4. ^{1}H NMR spectra of (a) EDTP ester (b) EDTP-4Na, and (c) EDTP acid.

[Color figure can be viewed in the online issue, which is available at wileyonlinelibrary.com.]

(—N<u>C</u>H$_2$CH$_2$CO—) has a higher shift value than that close to the carbonyl group (C═O), because the stronger electron-withdrawing effect of nitrogen (N) could reduce the electron shielding effect. This result indicates the existence of the ester bond in the as-synthesized EDTP ester. In addition, the peak characteristic of methoxy groups (at 3.67 ppm) exists in spectrum of EDTP ester (Figure 4a) but disappears in the spectrum of EDTP-4Na (Figure 4b), indicating that ester bonds of EDTP ester have been hydrolyzed completely and converted to EDTP-4Na successfully, under a strong alkaline condition.[38] Results of ^{13}C NMR in Figure 5 also confirm the successful hydrolysis since the characteristic peak of the methoxy group (O<u>C</u>H$_3$) located at 49.76 ppm in spectra of EDTP ester (Figure 5a) cannot be observed in that of EDTP-4Na (Figure 5b). Based on above results, it can be concluded that the ester groups (—COOCH$_3$) in EDTP ester has been fully converted into carboxylate groups in EDTP-4Na. The characteristic peaks are summarized in the Supporting Information in details.

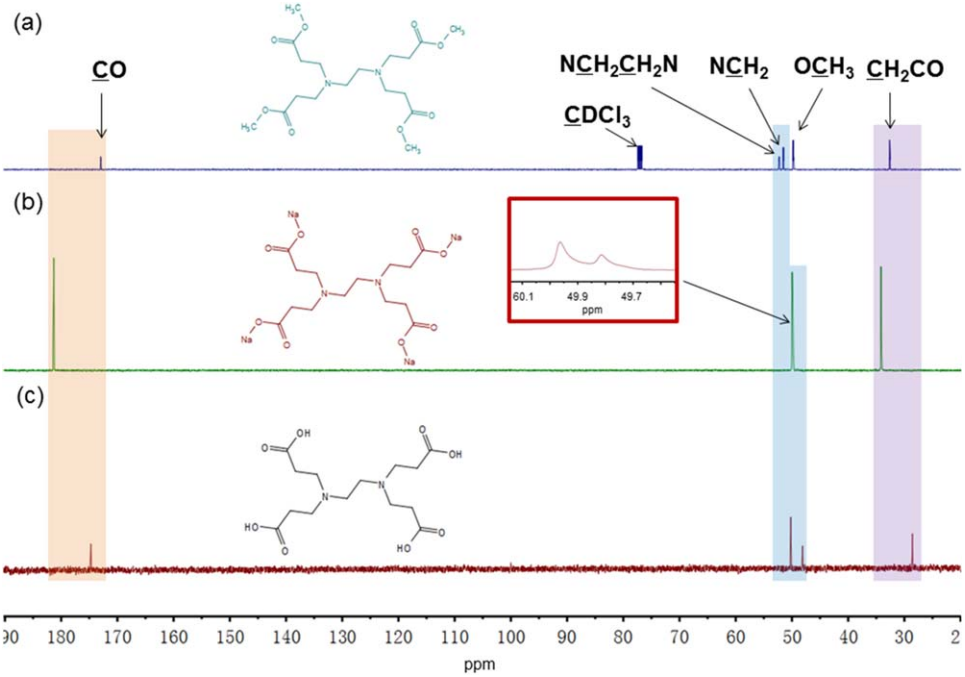

Figure 5. ^{13}C NMR spectra of (a) EDTP ester, (b) EDTP-4Na, and (c) EDTP acid.

[Color figure can be viewed in the online issue, which is available at wileyonlinelibrary.com.]

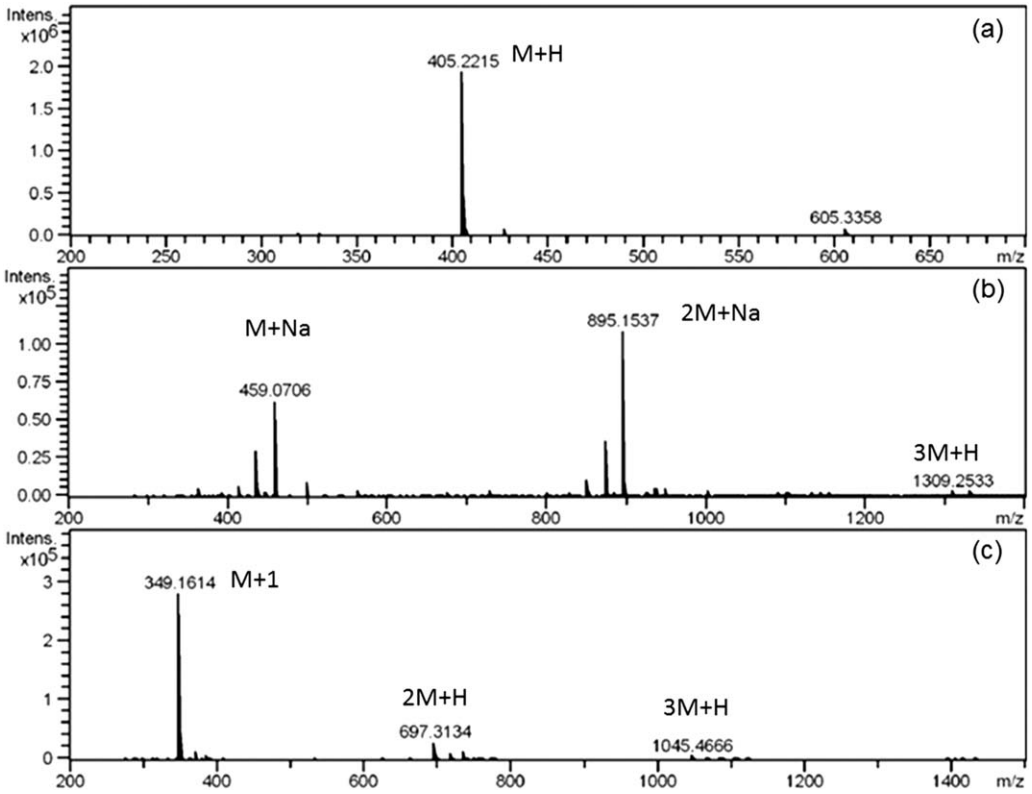

Figure 6. High resolution mass spectra of (a) EDTP ester, (b) EDTP-4Na, and (c) EDTP acid.

However, since NMR cannot detect the hydrogen on carboxyl groups, the difference between EDTP-4Na and EDTP acid cannot be observed well using above characterization techniques. Further verification of the hydrolysis process is established by HRMS. The HRMS spectra in Figure 6 reveals that molecular weights of the obtained EDTP ester (M+H), EDTP-4Na (M+Na), and EDTP acid (M+H) are 405.2215, 459.0706, and 349.1614, which agree very well with their theoretical molecular weights of 405.2237, 459.0708, and 349.1611, respectively.

In addition, FTIR spectra displayed in Figure 7 also exhibits the similar structural evolution of the EDTP compound from ester to salt to acid. The characteristic peak located at 1738 cm^{-1} can be attributed to the lattice absorption of carbonyl groups (C═O), while the peak around 1198 cm^{-1} is contributed by the stretching vibration of carboxyl groups (—COO^-). Besides, the peaks at 1462 and 1412 cm^{-1} of the C—H vibration and at 724 cm^{-1} of the C—H in-plane rocking vibration further confirm the presence of methylene groups (CH_2). The characteristic absorption bands centered at ~2953 and 2828 cm^{-1} are caused by C—H stretching in CH_2 and CH_3 groups. The above characteristic absorptions indicate that EDTP ester was formed successfully. In addition, it is noted that the peak (at 2828 cm^{-1}) of CH_3 groups disappears in the spectra of EDTP salt and acid, suggesting that the hydrolysis reaction from EDTP ester to EDTP acid is complete. The weak broad peak located at ~3455 cm^{-1} also indicates the successful formation of the O—H bonds in EDTP acid.[42]

Optimization of the pH value of the EDTP sodium solution

Despite that EDTP-4Na owns a good water solubility and generates a high osmotic pressure in the aqueous solution, which result in a superior water flux in FO process, the high pH of pure EDTP-4Na draw solution has a severe impact on the stability of the CTA membrane and may lead to a high reverse salt flux (see in Supporting Information, Figure S1). This phenomenon may be due to the hydrolysis reaction on the selective layer of CTA membrane under an extortionate pH condition (up to 12.33). On the other side, the pH of 0.2 M EDTP acid solution is around 2, which is beyond the pH tolerance limit of the CTA membrane (3–8).[43] EDTP acid also has a poor solubility in water. Therefore, both EDTP-4Na and EDTP acid were not suitable to be used as the draw solution alone.

By adjusting the solution pH to a suitable value, the balance between a good water solubility of the draw solute, an acceptable pH to the membrane, and therefore, a good FO performance can be achieved. As well known, generally the ion or hydrogen bond is the original root of the osmotic pressure. If a compound is fully dissolved in water, it can generate lots of ions or hydrogen bonds resulting in a high osmotic pressure. According to Table 2, the pH values of 0.2 M solution of EDTP-4Na and EDTP acid are 12.33 and 1.99, respectively. More specifically, the as-prepared draw solution is a multicomponent mixture, where the contents of EDTP acid, EDTP-Na, EDTP-2Na, EDTP-3Na, and EDTP-4Na experience a regular variation with pH increasing from 5.5 to 9, as displayed in Figure 8. To investigate the components' distribution in the mixture solution, the dissociation constants (p*K*a)[41] and pH of EDTP acid are introduced to calculate the distribution coefficients of 0.2 M EDTP sodium salts (details provided in the Supporting Information). It can be seen that concentrations of EDTP-3Na and EDTP-4Na salts in the total EDTP content increase from 14.48 and 0% to 92.29 and 2.31%, respectively, when the solution pH

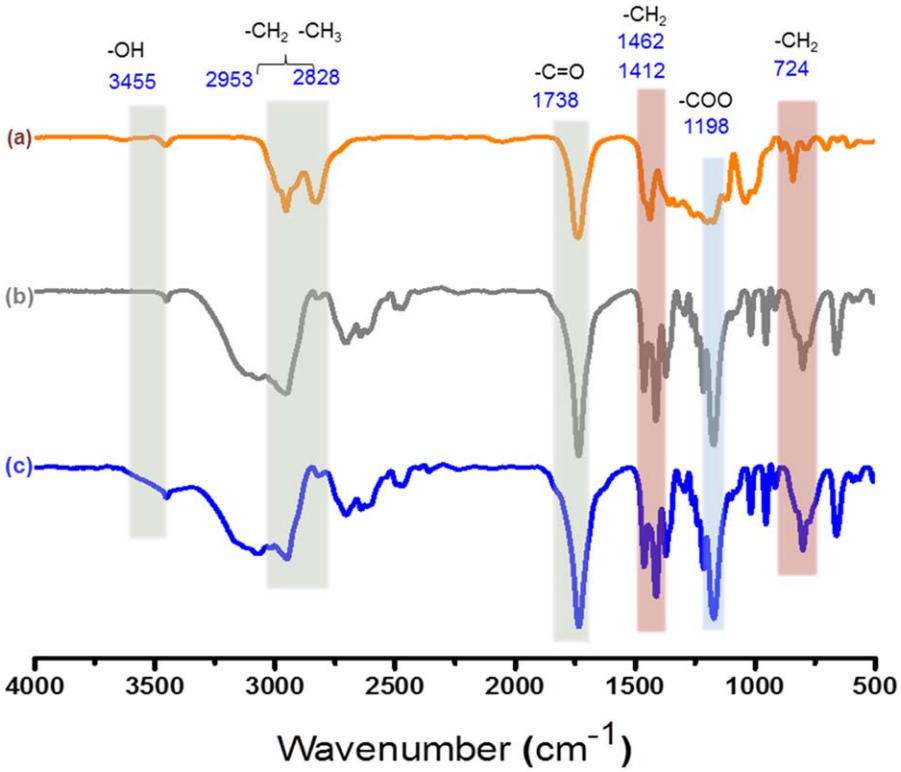

Figure 7. FT-IR spectra of (a) EDTP ester (b) EDTP-4Na, and (c) EDTP acid.

[Color figure can be viewed in the online issue, which is available at wileyonlinelibrary.com.]

increases from 6 to 8. But the content of EDTP-2Na decreases from 84.87 to 0% when the pH varies from 5.5 to 9. In addition, the contents of EDTP acid and EDTP-Na drop to zero as pH value exceeds 6.5. Clearly, the EDTP-2Na and EDTP-3Na salts are the main contents of the solution. For instance, the 0.2 M solution at pH of 8 contains 92.25% EDTP-3Na, 5.44% EDTP-2Na, and 2.31% EDTP-4Na.

Because FO process is an osmotically driven membrane process, the osmotic pressure of the used draw solution is a critical parameter to determine the water flux in the FO process. For simple inorganic compounds as draw solutes (e.g., NaCl and $MgCl_2$),[44] their osmotic pressures can be easy calculated by van't Hoff empirical formula or commercial software (OLI Stream Analyzer).[45] But for complex compounds (e.g., 2-methylimidazole-based compounds,[46] polyelectrolytes,[40,47] or magnetic particles,[33,48]) it is difficult to estimate the osmotic pressure by above methods. In previous works, osmometer is frequently used to determine the osmotic pressure of draw solutions.[29,47] In one recent work, the freezing point depression method was also used by Duan et al.[40] to measure the osmotic pressure of the polyelectrolyte draw

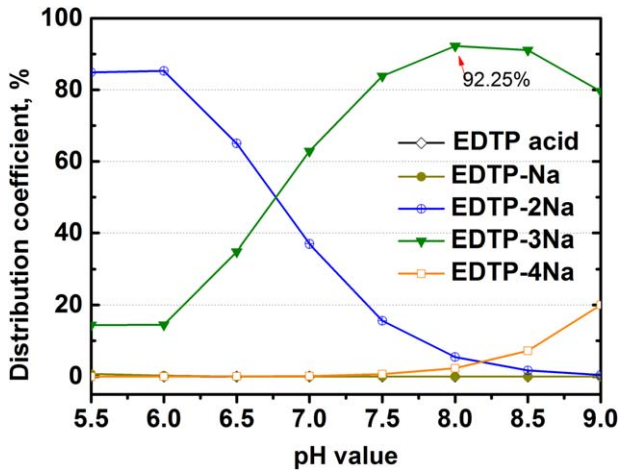

Figure 8. The distribution coefficients of each component in EDTP solution (0.2 M) with various pH values.

[Color figure can be viewed in the online issue, which is available at wileyonlinelibrary.com.]

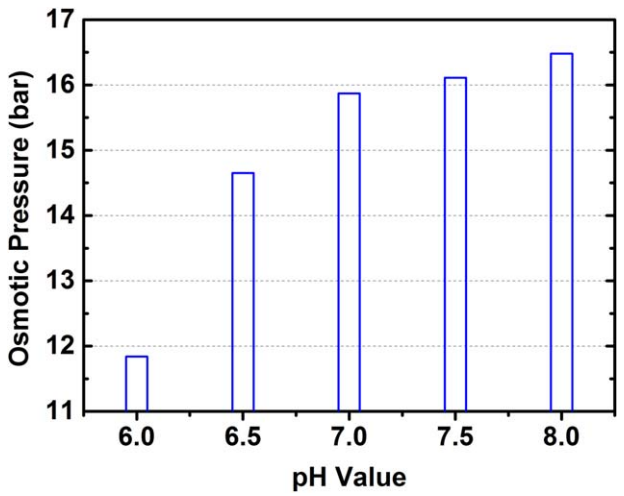

Figure 9. Effects of pH value on the osmotic pressure of EDTP solution (0.2 M).

[Color figure can be viewed in the online issue, which is available at wileyonlinelibrary.com.]

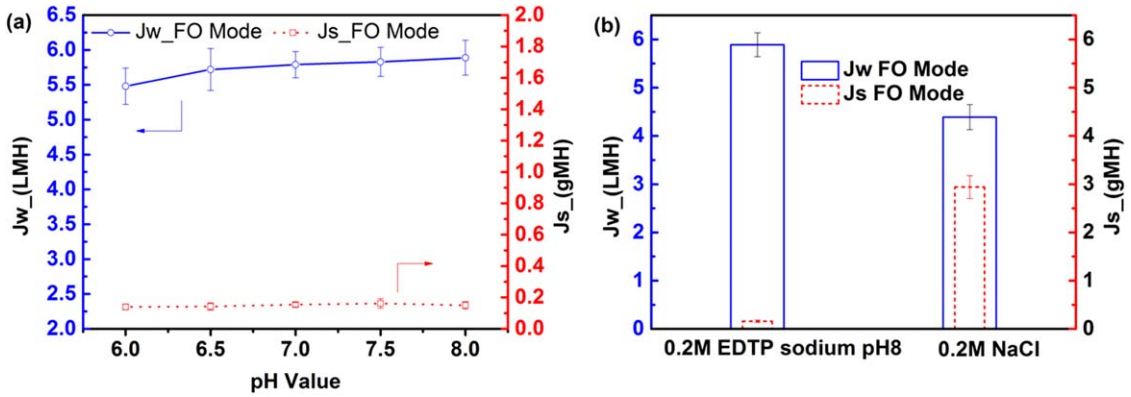

Figure 10. (a) Effects of pH value on the water flux and salt flux with EDTP solution (0.2 M) as the draw solution in FO mode; (b) Comparison of the water flux and salt flux with 0.2 M EDTP solution (pH of 8) and NaCl solution as the draw solution in FO mode.

[Color figure can be viewed in the online issue, which is available at wileyonlinelibrary.com.]

solute directly. In this work, the osmotic pressures of draw solutions with various pHs (from 6 to 8) are measured by the same method, and the result is shown in Figure 9. It shows an increasing trend with the increase in the solution pH, because of the increment in the free ion number.

To further explore the potential of EDTP as the draw solute, the pH effect of EDTP sodium solution on the resultant FO performance is evaluated, as shown in Figure 10. The water flux is recorded in FO mode. Figure 10a shows that water flux increases slowly with the increasing pH in the draw solution, which is consistent with the trend of the osmotic pressure. However, the salt leakage shows a slight increase (0.14–0.16 gMH) in the pH range of 6–7.5 and then a slight decreases at pH 8. The possible reason of the severer salt leakage is due to the increased free ions in the draw solution with the increasing pH value (6–7.5), leading to more free ions into the feed solution. According to the reported literature, the sodium ion with a hydrated radius of 0.36 nm[49] is able to pass through the membrane with a mean pore radius of 0.37 nm[50] into the feed solution under a low pH of 6–7.5. But under a higher pH condition, sodium ions' permeation from the draw solution to the feed solution will be limited to maintain the charge balance according to the Donnan equilibrium effect.[51] Besides, $EDTP^{3-}$ ions, the main component (92.25 %) in the EDTP solution at pH of 8, exhibit more charge in the draw solution than others except $EDTP^{4-}$, and could not pass through the FO membrane (CTA) easily. The combined effect of the above factors cause the resultant decline in the salt leakage at pH 8. With 0.2 M, EDTP draw solution at pH 8 for FO process, a water flux up to 5.89 ± 0.25 LMH could be obtained, which is much higher than that with 0.2 M NaCl as draw solution (4.39 ± 0.25 LMH), together with a lower salt flux of 0.16 ± 0.02 gMH than that with NaCl draw solution (2.94 ± 0.24 gMH), as shown in Figure 10b.

Effect of Draw Solute Concentration on FO Performance. As discussed above, the EDTP draw solution with optimized pH and solubility could exhibit a great potential for FO application. This could be proved by its outstanding osmotic pressure as compared with conventional NaCl and EDTA draw solutions as shown in Figure 11. Different with the linear increasing trend of the osmotic pressure of EDTA and NaCl draw solutions with the concentration increase, the osmotic pressure of EDTP draw solution has an exponentially increasing trend. Despite NaCl are strong electrolytes, since EDTP salt contains more carboxyl groups, the number of ions contained in EDTP draw solution is much higher than that of NaCl with the same mole concentration, resulting in a much higher osmotic pressure than that of NaCl, as shown in Figure 11. As compared with EDTA draw solution, in spite of their similar chemical structures, their physicochemical properties could be significantly different. It is noted that a larger amount of NaOH is consumed with EDTP acid solution than that with EDTA acid in the preparation of draw solutions with the same concentration and pH 8, indicating again that the former has more ions than the later.

Figure 12 presents the effect of draw solution concentration on the water flux (J_w) and salt flux (J_s) under both FO and PRO modes. As expected, the water fluxes with EDTP draw solution are higher than those with EDTA and NaCl, in both FO and PRO modes. Here the FO performance with EDTA draw solutions of 0.1–0.8 M at PRO mode is similar with that in the reported literature.[28] In addition, the water fluxes in PRO mode are all higher than those in FO mode.[52,53] This is because that the ICP in the porous CTA

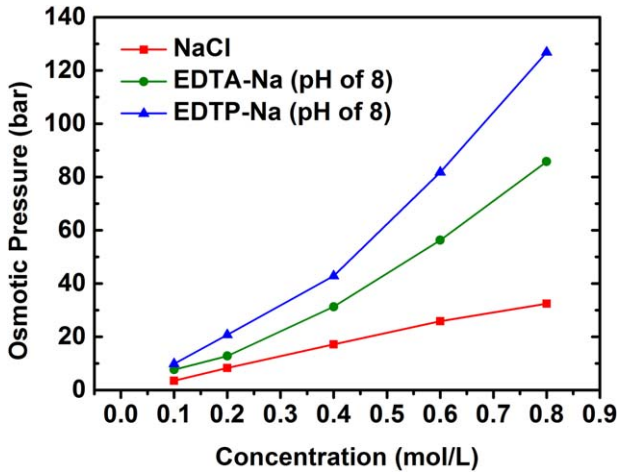

Figure 11. Effects of draw solute concentration on the osmotic pressure.

[Color figure can be viewed in the online issue, which is available at wileyonlinelibrary.com.]

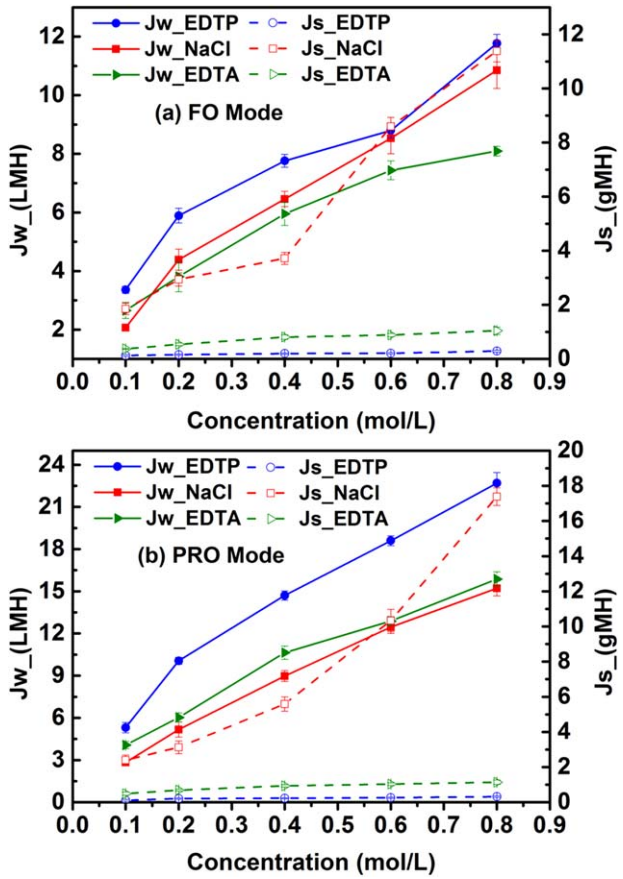

Figure 12. FO performance with EDTP sodium salt, EDTA sodium salt and NaCl as draw solute in (a) FO mode and (b) PRO mode. (Feed: DI water; membrane: commercial HTI-CTA FO membranes).

[Color figure can be viewed in the online issue, which is available at wileyonlinelibrary.com.]

support layer is much severer in FO mode, which reduces the net osmotic driving force and leads to a lower water flux.[23,54] Figure 12 also shows that, when the solute concentration increases from 0.1 to 0.8 M, the water flux also increases from 3.36 to 11.77 LMH in FO mode (Figure 12a), while from 5.31 to 22.69 LMH in PRO mode (Figure 12b). Basically this trend is consistent with the change of the osmotic pressure with the concentration change (Figure 11), but no exponential growth trend is observed as that of the osmotic pressure. This is probably caused by the existence of the ICP in FO mode,[55] which cause the decline of the water flux at high draw solute concentration. With regard to the reverse salt flux, a slight growth trend is also observed in both FO and PRO modes owning to more free sodium ions with the increasing EDTP sodium concentration.

With regard to the reverse salt flux with EDTP draw solution, they are all significantly lower than those with EDTA and NaCl solutions, mainly because of the much bigger molecular size of the EDTP compound. A slight growth trend is also observed in both FO and PRO modes owning to more free sodium ions with the increasing EDTP sodium concentration. The maximum salt flux was found at the concentration of 0.8 M in both FO and PRO modes, where that in the former is slightly lower (0.29 gMH) than that in the later (0.32 gMH).

The ratio of salt flux to water flux (J_s/J_w) is generally used as a performance index to evaluate the draw solute leakage and the FO performance. Figure 13 compares the J_s/J_w ratios under FO and PRO modes with various draw solution concentrations. The results show that the J_s/J_w ratios in the FO test with EDTP draw solutes are all lower than 0.027 and 0.016 g L^{-1} in FO and PRO modes, respectively, indicating a much lower leakage than those with conventional NaCl draw solution (in the range of 0.61–1.14 g L^{-1}). Therefore, the FO test with EDTP sodium as draw solute show superior FO performance to that with conventional EDTA and NaCl draw solute, not only in terms of higher water fluxes, but also lower salt leakage. The great potential of EDTP sodium salts as draw solutes for FO application is highly expected.

Most engineering osmosis in industrial applications are for high salinity cases, which is beyond RO capability.[10] Draw solutions with high concentrations are also generally preferred to obtain a high osmotic pressure, and therefore, a high water flux.[10] Currently, most FO research works are with the draw solution concentration ranging from 0.1 to 1.0 M, or 0.02–720 g L^{-1}, or 9.3–60 wt %[22,28,30,36,40,56–58] (See Table S1 in the Supporting Information). However, the draw solution with a high concentration generally suffers high viscosity causing a severe concentration polarization in FO process.[10] In this work, EDTP draw solutions of 0.1–0.8 M (0.042–0.34 g mL^{-1} or 4–30 wt %) were used. The highest viscosity is about 4.4 of 0.8 M EDTP draw solution, which is still far lower than most other reported works[29,30,36,56] (See Table S2 in the Supporting Information). This indicates the great potential of the novel EDTP draw solution for FO applications from another aspect.

Stability and recovery of EDTP draw solution

Stability of the draw solution is an important parameter for FO application.[11] If the draw solute experiences biodegradation[20,21,59] or agglomeration[31] during FO tests, its osmotic pressure may drop significantly, leading to a reduced water flux. In this study, a FO test is carried out to monitor the durability of the 0.2 M EDTP sodium solution at pH 8 at room temperature over a 15-day period, and the result is shown in Figure 14. It can be seen that water flux fluctuates

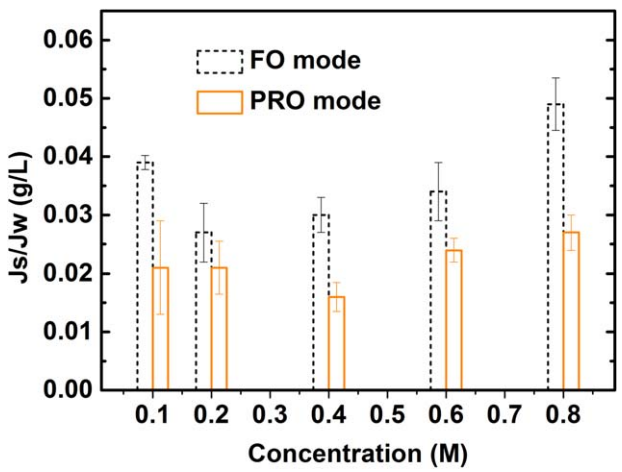

Figure 13. J_s/J_w ratios under FO and PRO modes with various draw solution concentrations.

[Color figure can be viewed in the online issue, which is available at wileyonlinelibrary.com.]

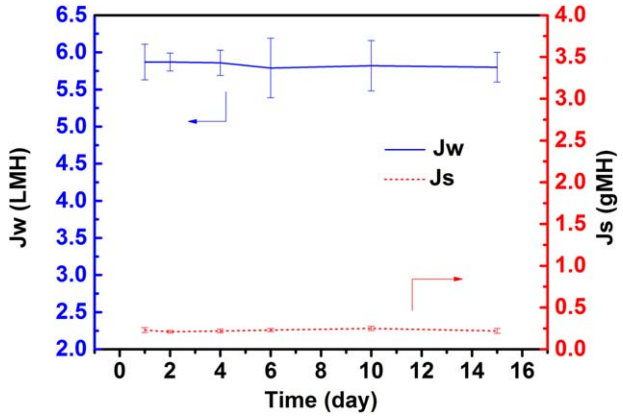

Figure 14. The assessment of CTA-membrane stability using 0.2 M EDTP draw solution under pH 8 for 15-day test.

[Color figure can be viewed in the online issue, which is available at wileyonlinelibrary.com.]

slightly in a range of 5.79–5.87 LMH and the salt flux remains quite constant within a range of 0.21–0.25 gMH. This result suggests that EDTP salt solution at pH 8 is quite stable and compatible well with the CTA membrane.

In FO process, because of the water transport and the draw solute leakage, the concentration of the draw solution may become more and more dilute, causing the sharp decline in its osmotic pressure and resultant water flux. The recovery of the draw solution is, therefore, a critical issue not only for the replenishment of the draw solution but also for the harvest of clean water product.[9] Depending on the molecule weight and structural size of the draw solutes to be recycled, a low pressure-driven membrane-based separation process, including NF,[60,61] UF,[48] and MD[59,62] can be used, which basically determines the energy consumption in FO reconcentration process. In other cases, using waste heat energy to recover the draw solutes (thermolytic salts)[23,25,26] could make FO an energy-efficient process.

For the NF recovery of the EDTP draw solution, a solute rejection about 71% is achieved. This solute rejection is relatively low mainly due to the fact that the NF membrane used in this work is only with a MWCO of 400 Da. As exhibited in Figure 8, the main components in the 0.2 M EDTP sodium solution at pH 8 are 92.25% $HEDTP^{3-}$ (Mw of 414), 5.44% H_2EDTP^{2-} (Mw of 392), and 2.11% $EDTP^{4-}$ (Mw of 436), respectively. As mentioned above, the feed solution in NF process to be recovered is 0.01 M EDTP solution diluted from the 0.2 M draw solution, where the percentages of $HEDTP^{3-}$ and $EDTP^{4-}$ will increase slightly because of their high dissociation degrees in the diluted solution. Those ions with molecular weights below or close to 400 Da (H_2EDTP^{2-} and $HEDTP^{3-}$) may pass through the NF membrane, leading to a relative low rejection. Despite that FO is not an energy efficient process when it is coupled with RO/NF process,[10] this work is just a conceptual study of the EDTP compound as the potential draw solute in FO application. To improve the energy efficiency, some possible approaches may be used to solve this problem. One is to develop draw solutes with bigger molecular size, so they could be recovered with lower energy-consumptive filtration process; the other is to use other energy-saving technologies, such as eutectic freezing crystallization technology[63,64] for the concentration of aqueous salt solutions. Besides, some other novel draw solutes, such as thermolytic salts,[23–26] magnetic nanoparticles,[31] and thermoresponsive polymer,[32] could also be regenerated by solar-light or magnetic field in an energy-saving process.

Conclusion

In this work, a novel draw solute with EDTP acid/salt with tetra-carboxyl groups is successfully synthesized, characterized and applied for FO application. The effects of solution pH and concentration on the osmotic pressure and resulted FO performance are systematically studied. The following conclusions can be drawn from this work:

1. EDTP acid with tetra-carboxyl structure has been successfully synthesized through a simple three-step reaction. NMR, HRMS, and FT-IR are used to confirm the structural evolution from EDTP ester to EDTP-4Na to EDTP acid.

2. With pH optimization, the improved solubility of EDTP sodium salts greatly enhances the osmotic pressure of the draw solution. The components in the EDTP mixture solution experience different distribution changes when the pH increases from 6 to 8. In the EDTP solution at pH 8, the main EDTP component is EDTP-3Na with a composition of about 92.25%. The osmotic pressure and FO performance also exhibit significant improvement with the pH increase.

3. Different with the traditional draw solution, the osmotic pressure of EDTP solution shows an exponential growth with the increase in its concentration, which contributes to the great enhancement of the water flux, particularly in PRO mode. A high water flux of 22.69 LMH and a low salt flux of 0.32 gMH can be achieved for 0.8 M EDTP sodium draw solution at pH 8 in the PRO mode. In addition, negligible J_s/J_w ratios ($\leq$0.05 g L^{-1}) can be achieved in both FO and PRO modes with the EDTP draw solution.

4. The developed EDTP compound has shown a good stability for a 15-day FO test and can be easily recovered by NF process. Further studies on EDTP compounds with bigger molecular size and improved solubility should be devoted and believed to hold good development prospect as draw solutes for future FO industrialization.

Acknowledgments

The authors thank the financial support from Huazhong University of Science and Technology China (Grant nos. 0124013041, 2013QN157, 2014YQ012), National Natural Science Foundation of China (Grant no. 21306058), and "Thousand Youth Talent Plan." Special thanks are due to Mr. Huayong Luo, Mr. Liang Shen, and Ms. Shu Xiong for their valuable help.

Notation

A = effective membrane surface area, m^2
C_0 = initial salt concentration of the feed, g L^{-1}
C_f = solute concentration in the feed solution, mol L^{-1}
C_p = solute concentration in the permeate, mol L^{-1}
C_t = salt concentration of the feed after the operation time interval, g L^{-1}
J_s = salt flux, g $m^{-2}h^{-1}$
J_w = water flux, L m^{-2} h^{-1}
m_0 = feed mass at time 0, kg
m_1 = feed mass after time t, kg
M = molar concentration, mol L^{-1}
Mw = weight-average molecular weight, g mol^{-1}
Δm = weight change in time t, kg
pKa = acid dissociation constants

R_s = solute rejection, %
t = time interval, h
T_0 = pure solvent freezing point temperature, °C
T_1 = solution freezing point temperature, °C
Δt = the operation time interval, h
ΔT = freezing point depression, °C
V_0 = initial volume of the feed, L
Vt = volume of the feed after the operation time interval, L.

Greek letters

π = osmotic pressure, bar
ρ = density, kg L^{-1}.

Abbreviations

DI = deionized
ECP = external concentration polarization
FO = forward osmosis
FTIR = Fourier Transform Infrared spectroscopy
gMH = g m^{-2} h^{-1}
HRMS = high resolution mass spectrum
ICP = internal concentration polarization
LMH = L m^{-2} h^{-1}
MWCO = molecular weight cut off, Da
NF = nanofiltration
NMR = nuclear magnetic resonance spectroscopy
PRO = pressure retarded osmosis
UF = ultrafiltration.

Literature Cited

1. Strathmann H. Membrane separation processes. *J Membr Sci*. 1981; 9:121–189.
2. Sun AC, Kosar W, Zhang YF, Feng XS. Vacuum membrane distillation for desalination of water using hollow fiber membranes. *J Membr Sci*. 2014;455:131–142.
3. Shao L, Cheng XQ, Liu Y, Quan S, Ma J, Zhao SZ, Wang KY. Newly developed nanofiltration (NF) composite membranes by interfacial polymerization for Safranin O and Aniline blue removal. *J Membr Sci*. 2013;430:96–105.
4. Li G, Li XM, Wang D, He T, Gao CJ. Forward osmosis membranes and applications. *Chem Ind Eng Prog*. 2010;8:1388–1398.
5. Fang YY, Bian LX, Wang XL. Understanding membrane parameters of a forward osmosis membrane based on nonequilibrium thermodynamics. *J Membr Sci*. 2013;437:72–81.
6. Su JC, Ong RC, Wang P, Chung T-S, Helmer BJ, de Wit JS. Advanced FO membranes from newly synthesized CAP polymer for wastewater reclamation through an integrated FO-MD hybrid system. *AIChE J*. 2013;59:1245–1254.
7. Elimelech M, Phillip WA. The future of seawater desalination: energy, technology, and the environment. *Science* 2011;333(6043): 712–717.
8. Elimelech M. Yale constructs forward osmosis desalination pilot plant. *Membr Technol*. 2007;2007:7–8.
9. Cath TY, Childress AE, Elimelech M. Forward osmosis: principles, applications, and recent developments. *J Membr Sci*. 2006;281:70–87.
10. Shaffer DL, Werber JR, Jaramillo H, Lin SH, Elimelech M. Forward osmosis: where are we now? *Desalination* 2015;356:271–284.
11. Ge QC, Ling MM, Chung T-S. Draw solutions for forward osmosis processes: developments, challenges, and prospects for the future. *J Membr Sci*. 2013;442:225–237.
12. Wang KY, Chung T-S, Amy G. Developing thin-film-composite forward osmosis membranes on the PES/SPSf substrate through interfacial polymerization. *AIChE J*. 2012;58:770–781.
13. Saren Q, Qiu CQ, Tang CY. Synthesis and characterization of novel forward osmosis membranes based on layer-by-layer assembly. *Environ Sci Technol*. 2011;45:5201–5208.
14. Flanagan MF, Escobar IC. Novel charged and hydrophilized polybenzimidazole (PBI) membranes for forward osmosis. *J Membr Sci*. 2013;434:85–92.
15. Zuo GZ, Wang R. Novel membrane surface modification to enhance anti-oil fouling property for membrane distillation application. *J Membr Sci*. 2013;447:26–35.
16. Setiawan L, Wang R, Li K, Fane AG. Fabrication of novel poly(amide-imide) forward osmosis hollow fiber membranes with a positively charged nanofiltration-like selective layer. *J Membr Sci*. 2011; 369:196–205.
17. Fang YY, Bian LX, Bi QY, Li Q, Wang XL. Evaluation of the pore size distribution of a forward osmosis membrane in three different ways. *J Membr Sci*. 2014;454:390–397.
18. Venault A, Chang Y, Wang D-M, Lai J-Y. Surface anti-biofouling control of PEGylated poly(vinylidene fluoride) membranes via vapor-induced phase separation processing. *J Membr Sci*. 2012;423–424:53–64.
19. Sukitpaneenit P, Chung T-S. High performance thin-film composite forward osmosis hollow fiber membranes with macrovoid-free and highly porous structure for sustainable water production. *Environ Sci Technol*. 2012;46:7358–7365.
20. Zhao SF, Zou LD, Tang CY, Mulcahy D. Recent developments in forward osmosis: opportunities and challenges. *J Membr Sci*. 2012; 396:1–21.
21. Su JC, Chung T-S. Sublayer structure and reflection coefficient and their effects on concentration polarization and membrane performance in FO processes. *J Membr Sci*. 2011;376:214–224.
22. Lutchmiah K, Lauber L, Roest K, Harmsen DJ, Post JW, Rietveld LC, Lier JB, Cornelissen ER. Zwitterions as alternative draw solutions in forward osmosis for application in wastewater reclamation. *J Membr Sci*. 2014;460:82–90.
23. McCutcheon JR, McGinnis RL, Elimelech M. Desalination by ammonia–carbon dioxide forward osmosis: influence of draw and feed solution concentrations on process performance. *J Membr Sci*. 2006;278:114–123.
24. McGinnis RL, McCutcheon JR, Elimelech M. A novel ammonia–carbon dioxide osmotic heat engine for power generation. *J Membr Sci*. 2007; 305:13–19.
25. Boo C, Khalil YF, Elimelech M. Performance evaluation of trimethylamine carbon dioxide thermolytic draw solution for engineered osmosis. *J Membr Sci*. 2015;473:302–309.
26. Yong JS, Phillip WA, Elimelech M. Reverse permeation of weak electrolyte draw solutes in forward osmosis. *Ind Eng Chem Res*. 2012;51:13463–13472.
27. Ge QC, Chung T-S. Hydroacid complexes: a new class of draw solutes to promote forward osmosis (FO) processes. *Chem Commun*. 2013;49:8471–8473.
28. Hau NT, Chen S-S, Nguyen NC, Huang KZ, Ngo HH, Guo WS. Exploration of EDTA sodium salt as novel draw solution in forward osmosis process for dewatering of high nutrient sludge. *J Membr Sci*. 2014;455:305–311.
29. Stone ML, Wilson AD, Harrup MK, Stewart FF. An initial study of hexavalent phosphazene salts as draw solutes in forward osmosis. *Desalination*. 2013;312:130–136.
30. Ge QC, Su JC, Amy GL, Chung T-S. Exploration of polyelectrolytes as draw solutes in forward osmosis processes. *Water Res*. 2012;46: 1318–1326.
31. Ling MM, Wang KY, Chung T-S. Highly water-soluble magnetic nanoparticles as novel draw solutes in forward osmosis for water reuse. *Ind Eng Chem Res*. 2010;49:5869–5876.
32. Li D, Zhang XY, Yao JF, Simon GP, Wang HT. Stimuli-responsive polymer hydrogels as a new class of draw agent for forward osmosis desalination. *Chem Commun*. 2011;47:1710–1712.
33. Ling MM, Chung T-S, Lu XM. Facile synthesis of thermosensitive magnetic nanoparticles as "smart" draw solutes in forward osmosis. *Chem Commun*. 2011;47:10788–10790.
34. Ge QC, Su JC, Chung T-S, Amy G. Hydrophilic superparamagnetic nanoparticles: synthesis, characterization, and performance in forward osmosis processes. *Ind Eng Chem Res*. 2010;50:382–388.
35. Bowden KS, Achilli A, Childress AE. Organic ionic salt draw solutions for osmotic membrane bioreactors. *Bioresour Technol*. 2012; 122:207–216.
36. Zhao DL, Chen SC, Wang P, Zhao QP, Lu XM. A dendrimer-based forward osmosis draw solute for seawater desalination. *Ind Eng Chem Res*. 2014;53:16170–16175.
37. Beaudry E, Herron J, Lampi K. Forward osmosis pressurized device and process for generating potable water. *US Patent* 6,849,184; 2005.
38. Garcia-Gallego S, Rodriguez JS, Jimenez JL, Cangiotti M, Ottaviani MF, Munoz-Fernandez MA, Gomez R, Mata FJ. Polyanionic N-donor ligands as chelating agents in transition metal complexes: synthesis, structural characterization and antiviral properties against HIV. *Dalton Trans*. 2012;41:6488–6499.
39. Wang YM, Kong WL, Song YJ, Wang LY, Steinhoff G, Kong DL, Yu YT. Polyamidoamine dendrimers with a modified pentaerythritol core having high efficiency and low cytotoxicity as gene carriers. *Biomacromolecules* 2009;10:617–622.

40. Duan JT, Litwiller E, Choi S-H, Pinnau I. Evaluation of sodium lignin sulfonate as draw solute in forward osmosis for desert restoration. *J Membr Sci*. 2014;453:463–470.
41. Chaberek JS, Martell A. Stability of metal chelates. IV. N, N′-ethylenediaminediacetic acid and N, N′-ethylenediaminediacetic-N, N′-dipropionic acid. *J Am Chem Soc*. 1952;74:6228–6231.
42. Smith BC. Infrared Spectral Interpretation: A Systematic Approach, 1st ed. Florida: CRC press, 1998.
43. Stone ML, Rae C, Stewart FF, Wilson AD. Switchable polarity solvents as draw solutes for forward osmosis. *Desalination*. 2013;312: 124–129.
44. Achilli A, Cath TY, Childress AE. Selection of inorganic-based draw solutions for forward osmosis applications. *J Membr Sci*. 2010; 364:233–241.
45. Wilson AD, Stewart FF. Deriving osmotic pressures of draw solutes used in osmotically driven membrane processes. *J Membr Sci*. 2013; 431:205–211.
46. Yen SK, Mehnas Haja N F, Su ML, Wang KY, Chung T-S. Study of draw solutes using 2-methylimidazole-based compounds in forward osmosis. *J Membr Sci*. 2010;364:242–252.
47. Ou RW, Wang YQ, Wang HT, Xu TW. Thermo-sensitive polyelectrolytes as draw solutions in forward osmosis process. *Desalination*. 2013, 318, 48–55.
48. Ling MM, Chung T-S. Desalination process using super hydrophilic nanoparticles via forward osmosis integrated with ultrafiltration regeneration. *Desalination*. 2011;278:194–202.
49. Tansel B. Significance of thermodynamic and physical characteristics on permeation of ions during membrane separation: hydrated radius, hydration free energy and viscous effects. *Sep Purif Technol*. 2012; 86:119–126.
50. Kiso Y, Muroshige K, Oguchi T, Hirose M, Ohara T, Shintani T. Pore radius estimation based on organic solute molecular shape and effects of pressure on pore radius for a reverse osmosis membrane. *J Membr Sci*. 2011;369:290–298.
51. Galama AH, Post JW, Cohen Stuart MA, Biesheuvel PM. Validity of the Boltzmann equation to describe Donnan equilibrium at the membrane–solution interface. *J Membr Sci*. 2013;442:131–139.
52. Oh Y, Lee S, Elimelech M, Lee S, Hong S. Effect of hydraulic pressure and membrane orientation on water flux and reverse solute flux in pressure assisted osmosis. *J Membr Sci*. 2014;465:159–166.
53. Cui Y, Ge QC, Liu X-Y, Chung T-S. Novel forward osmosis process to effectively remove heavy metal ions. *J Membr Sci*. 2014;467: 188–194.
54. Mehta GD, Loeb S. Internal polarization in the porous substructure of a semipermeable membrane under pressure-retarded osmosis. *J Membr Sci*. 1978;4:261–265.
55. Tan CH, Ng HY. Revised external and internal concentration polarization models to improve flux prediction in forward osmosis process. *Desalination*. 2013;309:125–140.
56. Zhao DL, Wang P, Zhao QP, Chen NP, Lu XM. Thermoresponsive copolymer-based draw solution for seawater desalination in a combined process of forward osmosis and membrane distillation. *Desalination*. 2014;348:26–32.
57. Na Y, Yang S, Lee S. Evaluation of citrate-coated magnetic nanoparticles as draw solute for forward osmosis. *Desalination*. 2014; 347:34–42.
58. Guo CX, Zhao DL, Zhao QP, Wang P, Lu XM. Na^{+}_{-}functionalized carbon quantum dots: a new draw solute in forward osmosis for seawater desalination. *Chem Commun*. 2014;50:7318–7321.
59. Ge QC, Wang P, Wan CF, Chung T-S. Polyelectrolyte-promoted forward osmosis–membrane distillation (FO–MD) hybrid process for dye wastewater treatment. *Environ Sci Technol*. 2012;46:6236–6243.
60. Zhao SF, Zou LD, Mulcahy D. Brackish water desalination by a hybrid forward osmosis–nanofiltration system using divalent draw solute. *Desalination*. 2012;284:175–181.
61. Tan CH, Ng HY. A novel hybrid forward osmosis-nanofiltration (FO-NF) process for seawater desalination: draw solution selection and system configuration. *Desalin Water Treat*. 2010;13:356–361.
62. Wang KY, Teoh MM, Nugroho A, Chung T-S. Integrated forward osmosis–membrane distillation (FO–MD) hybrid system for the concentration of protein solutions. *Chem Eng Sci*. 2011;66:2421–2430.
63. Fujioka R, Wang LP, Dodbiba G, Fujita T. Application of progressive freeze-concentration for desalination. *Desalination*. 2013;319: 33–37.
64. Williams PM, Ahmad M, Benjamin SC, Oatley-Radcliffe DL. Technology for freeze concentration in the desalination industry. *Desalination*. 2015;356:314–327.

Manuscript received Aug. 3, 2014, and revision received Dec. 15, 2014.